Eur J Nucl Med Mol Imaging (2016) 43:1664–1672
DOI 10.1007/s00259-016-3333-5

ORIGINAL ARTICLE

# Ability of $^{18}$F-DOPA PET/CT and fused $^{18}$F-DOPA PET/MRI to assess striatal involvement in paediatric glioma

**Giovanni Morana[1] · Matteo Puntoni[2] · Maria Luisa Garrè[3] · Michela Massollo[4] · Egesta Lopci[5] · Merhdad Naseri[4] · Mariasavina Severino[1] · Domenico Tortora[1] · Andrea Rossi[1] · Arnoldo Piccardo[4]**

Received: 17 October 2015 / Accepted: 7 February 2016 / Published online: 25 February 2016


**Abstract**
*Purpose* To assess the diagnostic performance of $^{18}$F-DOPA PET/CT and fused $^{18}$F-DOPA PET/MRI in detecting striatal involvement in children with gliomas.
*Methods* This retrospective study included 28 paediatric patients referred to our institution for the presence of primary, residual or recurrent glioma (12 boys, 16 girls; mean age 10.7 years) and investigated with $^{18}$F-DOPA PET/CT and brain MRI. Fused $^{18}$F-DOPA PET/MR images were obtained and compared with PET/CT and MRI images. Accuracy, sensitivity, specificity, negative predictive value (NPV) and positive predictive value (PPV) for striatal involvement were calculated for each diagnostic tool. Univariate and multivariate logistic analyses were applied to evaluate the associations between $^{18}$F-DOPA PET/CT and fused $^{18}$F-DOPA PET/MRI diagnostic results and tumour uptake outside the striatum, grade, dimension and site of striatal involvement (ventral and/or dorsal).
*Results* Accuracy, sensitivity, specificity, PPV, and NPV were 100 % for MRI, 93 %, 89 %, 100 %, 100 % and 82 % for $^{18}$F-DOPA PET/MRI, and 75 %, 74 %, 78 %, 88 % and 58 % for $^{18}$F-DOPA PET/CT, respectively. $^{18}$F-DOPA PET/MRI showed a trend towards higher accuracy compared with $^{18}$F-DOPA PET/CT ($p = 0.06$). MRI showed significantly higher accuracy compared with $^{18}$F-DOPA PET/CT ($p = 0.01$), but there was no significant difference between MRI and $^{18}$F-DOPA PET/MRI. Both univariate and multivariate logistic analyses showed a significant association (OR 8.0 and 7.7, respectively) between the tumour-to-normal striatal uptake (T/S) ratio and the diagnostic ability of $^{18}$F-DOPA PET/CT ($p = 0.03$). A strong significant association was also found between involvement of the dorsal striatum and the $^{18}$F-DOPA PET/CT results ($p = 0.001$), with a perfect prediction of involvement of the dorsal striatum by $^{18}$F-DOPA PET/MRI.
*Conclusion* Physiological striatal $^{18}$F-DOPA uptake does not appear to be a main limitation in the evaluation of basal ganglia involvement.$^{18}$F-DOPA PET/CT correctly detected involvement of the dorsal striatum in lesions with a T/S ratio >1, but appeared to be less suitable for evaluation of the ventral striatum. The use of fused $^{18}$F-DOPA PET/MRI further improves the accuracy and is essential for evaluation of the ventral striatum.

**Keywords** F-DOPA PET/CT · $^{18}$F-DOPA PET/MRI · Striatum · Paediatric · Gliomas

✉ Arnoldo Piccardo
arnoldo.piccardo@galliera.it

[1] Neuroradiology Unit, Istituto Giannina Gaslini, Genova, Italy
[2] Clinical Trial Unit, Scientific Directorate, Ospedali Galliera, Genova, Italy
[3] Neuro-oncology Unit, Istituto Giannina Gaslini, Genova, Italy
[4] Nuclear Medicine Unit, E.O. Ospedali Galliera, Mura delle Cappuccine 14, 16128 Genoa, Italy
[5] Nuclear Medicine Unit, Humanitas Clinical and Research Hospital, Rozzano, Italy

## Introduction

PET imaging with amino acid analogues is increasingly being used for the evaluation and management of paediatric brain tumours. $^{11}$C-Methionine was the first probe used in children with brain malignancies [1, 2], but its short half-life (20 min) limits its use to centres with an on-site cyclotron. More recently, $^{18}$F-labelled tracers have gained importance because of their longer half-life (110 min) which has led to their

**Table 1** Summary of patient characteristics and imaging findings

| Patient | Sex | Age (years) | Diagnosis | WHO grade | Primary, residual, recurrent | Uptake ratios | | Striatal involvement (yes/no) | | | |
|---|---|---|---|---|---|---|---|---|---|---|---|
| | | | | | | Tumour to normal striatum | Tumour to normal brain region | PET/CT | PET/MRI | MRI | Gold standard[a] |
| 1 | F | 1 | PA | I | Primary | 1.36 | 2.10 | Yes | Yes | Yes | Yes |
| 2 | F | 13 | GG | I | Residual | 0.89 | 1.80 | No | No | Yes | Yes |
| 3 | M | 15 | GC (DA) | II | Primary | 0.85 | 1.34 | No | No | Yes | Yes |
| 4 | M | 12 | GC (DA) | II | Primary | 1.20 | 2.30 | Yes | Yes | Yes | Yes |
| 5 | F | 11 | DA | II | Primary | 0.80 | 1.57 | No | Yes | Yes | Yes |
| 6 | M | 2 | DA | II | Primary | 0.75 | 1.20 | No | No | No | No |
| 7 | M | 17 | DA | II | Primary | 0.80 | 1.40 | No | Yes | Yes | Yes |
| 8 | F | 17 | AGG | III | Recurrent | 1.33 | 1.59 | Yes | Yes | Yes | Yes |
| 9 | F | 6 | AA | III | Primary | 1.20 | 1.73 | No | Yes | Yes | Yes |
| 10 | M | 11 | GC (AA) | III | Primary | 1.23 | 1.72 | Yes | Yes | Yes | Yes |
| 11 | F | 11 | AA | III | Residual | 1.00 | 1.20 | Yes | Yes | Yes | Yes |
| 12 | M | 4 | DIPG | High grade | Primary | 1.20 | 2.00 | No | No | No | No |
| 13 | F | 16 | DIPG (AA) | III | Primary | 1.50 | 2.30 | No | No | No | No |
| 14 | F | 4 | DIPG | High grade | Primary | 1.00 | 1.70 | No | No | No | No |
| 15 | F | 7 | DIPG | High grade | Primary | 0.65 | 1.30 | No | No | No | No |
| 16 | M | 9 | AA | III | Primary | 2.50 | 2.90 | No | No | No | No |
| 17 | F | 11 | AA | III | Residual | 1.10 | 2.20 | Yes | Yes | Yes | Yes |
| 18 | F | 9 | AGG | III | Recurrent | 1.60 | 2.20 | Yes | Yes | Yes | Yes |
| 19 | M | 15 | AA | III | Recurrent | 1.77 | 2.75 | Yes | Yes | Yes | Yes |
| 20 | F | 17 | AA | III | Primary | 1.70 | 2.60 | Yes | Yes | Yes | Yes |
| 21 | F | 12 | GBM | IV | Recurrent | 0.86 | 1.30 | Yes | No | No | No |
| 22 | M | 8 | GBM | IV | Primary | 1.46 | 2.00 | Yes | Yes | Yes | Yes |
| 23 | F | 17 | GBM | IV | Residual | 1.15 | 2.30 | Yes | Yes | Yes | Yes |
| 24 | F | 7 | GBM | IV | Primary | 1.45 | 2.38 | Yes | No | No | No |
| 25 | M | 9 | GBM | IV | Primary | 1.70 | 2.80 | Yes | Yes | Yes | Yes |
| 26 | F | 15 | GBM | IV | Residual | 2.20 | 3.80 | Yes | Yes | Yes | Yes |
| 27 | M | 7 | GBM | IV | Primary | 1.00 | 1.70 | Yes | Yes | Yes | Yes |
| 28 | M | 16 | GBM | IV | Residual | 1.80 | 2.57 | No | No | No | No |

*PA* pilocytic astrocytoma, *GG* ganglioglioma, *GC* gliomatosis cerebri, *DA* diffuse astrocytoma, *DIPG* diffuse intrinsic pontine glioma, *AA* anaplastic astrocytoma, *AGG* anaplastic ganglioglioma, *GBM* glioblastoma multiforme

[a] Follow-up MRI studies

widespread use. Among them, $^{18}$F-dihydroxyphenylalanine (DOPA) has been found to be a multitargeted molecule in children, since it can be used for the evaluation of primary/recurrent brain tumours [3, 4], for the diagnosis, prognosis and surveillance of neuroblastoma [5, 6], including detection of CNS metastasis [7], and in nontumoral conditions such as congenital hyperinsulinism [8].

Recent data suggest that $^{18}$F-DOPA PET imaging in children with infiltrative glioma can add valuable diagnostic, prognostic and therapeutic information. Significant differences in $^{18}$F-DOPA uptake have been demonstrated between low-grade and high-grade lesions and $^{18}$F-DOPA uptake correlates significantly with outcome, both in terms of progression-free survival and overall survival [3, 9]. $^{18}$F-DOPA PET imaging is also useful for biopsy planning and posttreatment monitoring, and can contribute to the stratification of patients with diffuse astrocytoma and gliomatosis cerebri, thereby influencing their management [3]. Similar results have been reported for $^{18}$F-fluoroethyl-L-tyrosine ($^{18}$F-FET) [10, 11] and $^{18}$F-choline [12]. In particular, $^{18}$F-FET PET-guided surgical biopsy and resection [10] has been used to characterize undetermined brain lesions, detect tumour

recurrence and to evaluate treatment response [11]. However, the main potential drawback of $^{18}$F-DOPA compared with other fluorinated tracers is its specific uptake in the putamen and caudate nucleus that may affect the ability to assess involvement of the striatum.

On the basis of these considerations, the overall objective of this study was to evaluate the performance of $^{18}$F-DOPA PET/CT and fused $^{18}$F-DOPA PET/MRI in detecting striatal involvement in paediatric glioma.

## Materials and methods

### Patients

A retrospective review was conducted of all paediatric patients (aged between 1 and 18 years) referred to our Institution for the presence of primary, residual or recurrent brain gliomas (with or without prior treatment), who underwent MRI and $^{18}$F-DOPA PET within 2 weeks of each other. A total of 34 patients were identified, of whom 6 patients with lesions demonstrating negligible PET uptake and corresponding to histologically proven diffuse astrocytoma were excluded. The remaining 28 patients (12 boys and 16 girls) with brain glioma exhibiting tracer uptake above the level of normal background were included in the analysis. Patient ages ranged from 1 to 17 years (average 10.7 years). Diagnosis was histologically confirmed in all patients except three with diffuse intrinsic pontine glioma. The main characteristics of the patients and their brain lesions are summarized in Table 1. The Institutional Review Board approved the study.

### Imaging protocol and analysis

$^{18}$F-DOPA was purchased from a commercial supplier (IASOdopa; IASON Labormedizine Ges.Mbh & Co. KG). Data were acquired in three-dimensional mode on a dedicated PET/CT system (Discovery ST, GE Medical Systems) 20 min after injection of 185 MBq of $^{18}$F-DOPA in all patients (scan time 30 min). The patients fasted for at least 4 h before the $^{18}$F-DOPA PET scan. Carbidopa premedication was not utilized. A nondiagnostic, low-dose CT scan (120 kV, 80 mA, 0.6 s per rotation) was used for attenuation correction. MRI studies were performed on a 1.5-T magnet (Intera Achieva; Philips, Best, The Netherlands) and included axial fluid attenuation inversion recovery (FLAIR), T2-weighted and T1-weighted images, coronal FLAIR and T2-weighted images, and contrast-enhanced (gadolinium chelate, 0.1 mmol/kg) axial, coronal and sagittal T1-weighted images.

All $^{18}$F-DOPA PET/CT studies were first inspected visually. Then a circular region of interest (ROI) of 10 mm diameter was manually drawn over the tumour (T) area displaying the highest $^{18}$F-DOPA PET uptake outside the striatum. The radiotracer concentration in the ROI was normalized to the injected dose per patient body weight and the maximum standardized uptake value (SUVmax; grams per millilitre) was obtained for each lesion. For the normal background (N) reference tissue, a large ROI (diameter 50 mm) was drawn in the normal brain at the level of the centrum semiovale, including grey and white matter. An additional ROI (diameter 10 mm) was drawn over the normal striatum (S). Tumour to normal tissue uptake ratios were generated by dividing the tumour SUVmax by the SUVmax of the normal brain region (T/N) and of the normal striatum (T/S).

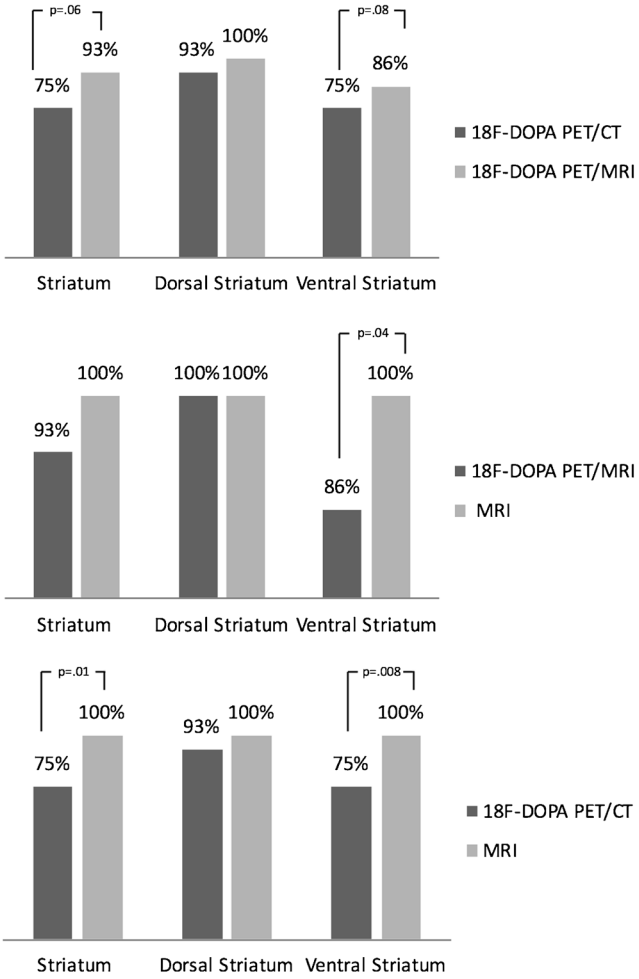


**Fig. 1** Patient-based analysis and detection of striatal involvement (accuracy) by $^{18}$F-DOPA PET/CT, fused $^{18}$F-DOPA PET/MRI and MRI

Images were analysed on a dedicated workstation (Xeleris, GE Corporation), which also allowed semiautomatic coregistration and fusion of $^{18}$F-DOPA PET and MRI images ($^{18}$F-DOPA PET images were fused with axial FLAIR and contrast-enhanced T1-weighted images). Three sets of images were analysed for each patient: PET/CT (image set A), MRI (image set B), and PET/MRI (image set C). Separately and independently, one experienced nuclear medicine physician and radiologist

(A.P.) evaluated image set A, and one experienced neuroradiologist (G.M.) evaluated image set B. Subsequently, in a second image reading session, both readers evaluated image set C. When the readers evaluated image set C, they had available image set B, the PET part of the PET/CT dataset, and the fused PET/MRI dataset. To minimize any recall bias, the reading sessions were separated by 4 weeks. Neither reader was aware of the results of other imaging studies, the results of the other reader, or the findings of histopathological examination. The images of each image set were evaluated in random order.

The striatum was segmented into two regions, ventral and dorsal, according to conventional anatomical definition [13]. In detail, the ventral striatum included the nucleus accumbens, the head of the caudate nucleus and the most ventral and basal regions of the putamen. The remaining part corresponded to the dorsal striatum. Striatal involvement was considered positive on: (1) MRI according to standard diagnostic criteria, including partial infiltration detectable on T2/FLAIR images, (2) $^{18}$F-DOPA PET/CT in the presence of asymmetrical uptake associated with modified striatal outline or in the presence of focal uptake exceeding the adjacent or contralateral striatal physiological tracer activity, and (3) fused $^{18}$F-DOPA PET/MRI in the presence of uptake exceeding that of the adjacent or contralateral striatal physiological tracer activity or in the presence of modified striatal outline corresponding to an MRI lesion. Focal increased uptake clearly corresponding to benign nontumoral MRI lesions (i.e. developmental venous anomalies, ischaemic areas, postsurgical changes) were not considered positive. The standard of reference was based on follow-up MRI studies performed every 3 months during the year following the PET study.

## Statistical analysis

Descriptive statistics included mean, standard deviation, median, percentiles, minimum and maximum for continuous factors and scores, and number and relative frequencies (%) for categorical factors.

Sensitivity, specificity, positive predictive value (PPV), negative predictive value (NPV) and accuracy (calculated as [(true positives) + (true negatives)]/total) were calculated and compared between the PET/CT, PET/MRI techniques and the gold standard, as previously defined (brain MRI). Fisher's exact test was used to compare independent diagnostic indicators (PPV, NPV) and the univariate associations among the PET/CT results, PET/MRI results and tumour grade, and T/S and T/N ratios and tumour diameter. The McNemar test was used to compare paired diagnostic indicators (sensitivity, specificity, accuracy). Logistic regression modelling was used to calculate odds ratios (OR) and the Wald test was used to estimate and test the association between PET/CT and PET/MRI true positive results and the other parameters considered: tumour grade, T/S and T/N ratios, tumour diameter, and site of striatal involvement (dorsal or ventral). Odds ratios from the

**Table 2** Univariate and multivariate analyses to test the associations between PET/CT and PET/MRI true-positive results and tumour grade, T/S and T/N ratios, tumour diameter and site of striatal involvement

| Factor | | PET/CT | | | PET/MRI | | |
|---|---|---|---|---|---|---|---|
| | | No. (%) of patients | Odds ratio ($p$ value) | Adjusted odds ratio[a] ($p$ value) | No. (%) of patients | Odds ratio ($p$ value) | Adjusted odds ratio[a] ($p$ value) |
| Grade | I/II | 7 (25) | 1.0 | 1.0 | 7 (25) | 1.0 | 1.0 |
| | III/IV | 21 (75) | 3.3 (0.2) | 3.1 (0.3) | 21 (75) | 1.2 (0.8) | 0.9 (0.9) |
| T/S ratio | ≤1 | 10 (36) | 1.0 | 1.0 | 10 (36) | 1.0 | 1.0 |
| | >1 | 18 (64) | 8.0 (0.03) | 7.7 (0.03) | 18 (64) | 3.9 (0.1) | 3.7 (0.1) |
| T/N ratio | ≤1.3 | 4 (14) | 1.0 | 1.0 | 4 (14) | 1.0 | 1.0 |
| | >1.3 | 24 (86) | 3.5 (0.3) | 3.3 (0.3) | 24 (86) | 6.0 (0.2) | 5.9 (0.2) |
| Maximum diameter (mm), median | <5-6.5 | 14 (50) | 1.0 | 1.0 | 14 (50) | 1.0 | 1.0 |
| | ≥56.5 | 14 (50) | 1.8 (0.5) | 2.2 (0.4) | 14 (50) | 2.5 (0.3) | 3.8 (0.1) |
| Involvement of dorsal striatum | No | 15 (54) | 1.0 | 1.0 | 15 (54) | Perfect prediction: all patients true-positive | |
| | Yes | 13 (46) | 78 (0.001) | 109 (0.001) | 13 (46) | | |
| Involvement of ventral striatum | No | 16 (57) | 1.0 | 1.0 | 16 (57) | 1.0 | 1.0 |
| | Yes | 12 (43) | 1.8 (0.4) | 1.4 (0.7) | 12 (43) | 6.4 (0.04) | 5.7 (0.08) |

[a] From a multivariate logistic model, adjusting for age and sex

multivariate models were adjusted for age and sex of the patients.

All analyses were conducted using STATA, version 13 (StataCorp, College Station, TX). Two-tailed probabilities are reported and a *p*-value of 0.05 was used to define nominal statistical significance.

## Results

Striatal involvement was correctly identified by MRI in 19 of the 28 patients, by fused $^{18}$F-DOPA PET/MRI in 17 patients, and by $^{18}$F-DOPA PET/CT in 14 patients. Striatal involvement was confirmed in 19 patients. Both the ventral and dorsal striatum were involved in six patients, only the ventral striatum in six and only the dorsal striatum in seven.

In the patient-based analysis, sensitivity, specificity, PPV, NPV and accuracy were of 100 % for MRI, 89 %, 100 %, 100 %, 82 % and 93 % for $^{18}$F-DOPA PET/MRI, and 74 %, 78 %, 88 %, 58 % and 75 % for $^{18}$F-DOPA PET/CT, respectively. MRI showed a significantly higher accuracy ($p = 0.01$) and NPV ($p = 0.04$) compared with $^{18}$F-DOPA PET/CT. $^{18}$F-DOPA PET/MRI showed a trend towards higher accuracy compared with $^{18}$F-DOPA PET/CT ($p = 0.06$; Fig. 1). No significant differences in diagnostic ability were observed between MRI and $^{18}$F-DOPA PET/MRI.

Four of five patients with striatal involvement not detected by PET/CT, and the two patients with striatal involvement not detected by PET/MRI showed with low-grade glioma characterized by relatively low DOPA uptake (T/S ratio <1, Table 1). In evaluation of involvement of the ventral striatum, MRI had significantly higher

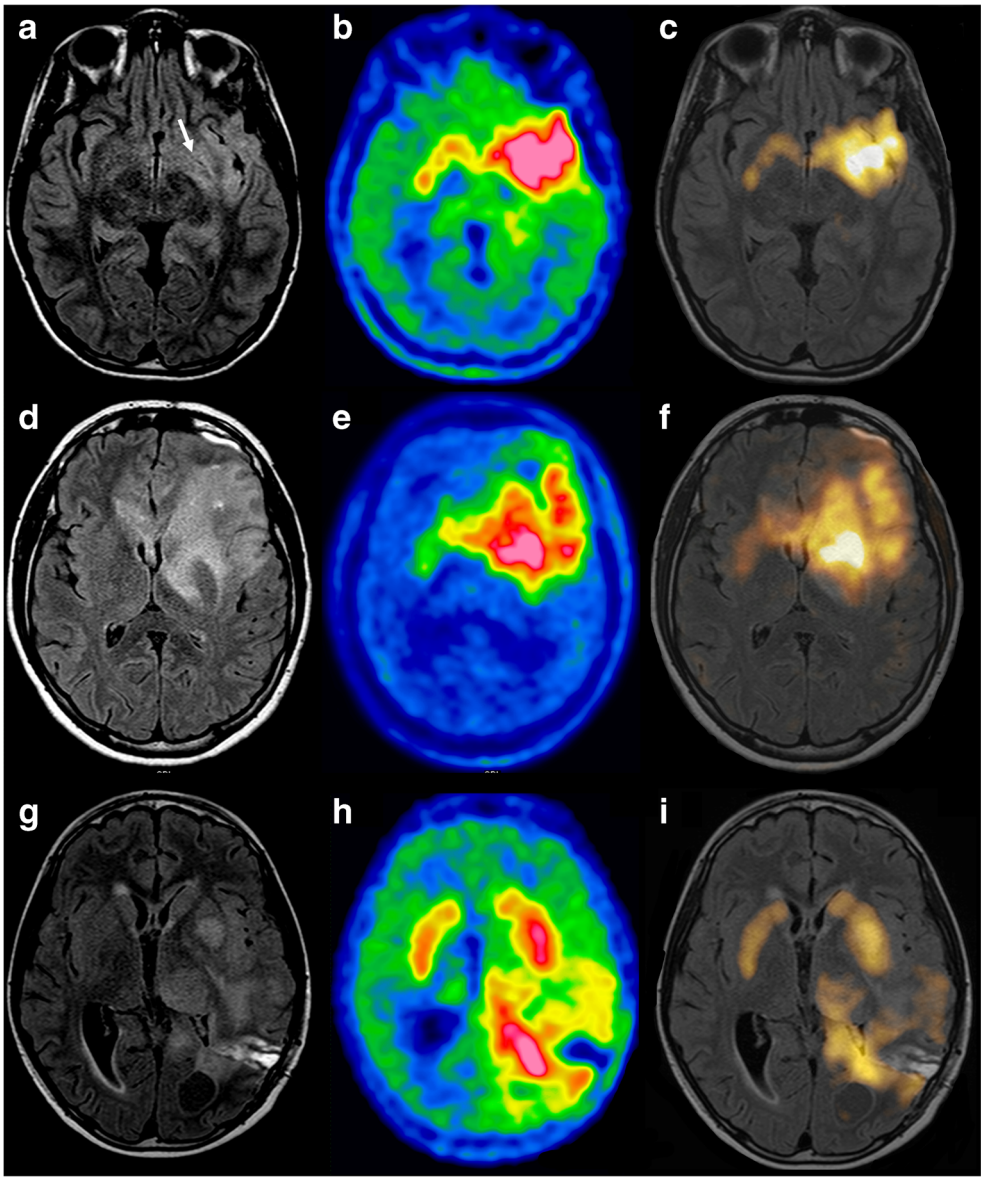


**Fig. 2** Positive $^{18}$F-DOPA PET/CT and $^{18}$F-DOPA PET/MRI images. **a–c** Glioblastoma multiforme (patient 26). The axial FLAIR image (**a**) shows a lesion in the left insula and temporal lobe involving the ipsilateral ventral striatum (*arrow*). The $^{18}$F-DOPA PET image (**b**) and fused PET/MRI image (**c**) clearly show asymmetrical uptake in the ventral striatum, greater on the left, matching the lesion on MRI. **d–f** Glioblastoma multiforme (patient 23). The axial FLAIR image (**d**) shows an extensive infiltrative lesion involving the left frontal and temporal lobe extending to the genu of the corpus callosum and to the ipsilateral ventral and dorsal striatum. The $^{18}$F-DOPA PET image (**e**) and fused PET/MRI image (**f**) show increased uptake and a modified outline of the left striatum. **g–i** Glioblastoma multiforme (patient 25). The axial FLAIR image (**g**) shows an extensive infiltrative lesion involving the left temporal-parietal lobe, the ipsilateral thalamus and the dorsal striatum (putamen). The $^{18}$F-DOPA PET image (**h**) and fused PET/MRI image (**i**) show increased uptake and a modified outline of the left putamen, matching the lesion on MRI

accuracy ($p = 0.008$), NPV ($p = 0.02$) and sensitivity ($p = 0.03$) than PET/CT and significantly higher accuracy than PET/MRI ($p = 0.04$). PET/MRI showed trend towards higher accuracy compared with PET/CT ($p = 0.08$; Fig. 1). In contrast, in evaluation of involvement of the dorsal striatum, there were no significant differences among PET/CT, PET/MRI and MRI (Fig. 1). Logistic regression analyses (Table 2) showed a significant association ($p = 0.03$) between T/S ratio and the ability of $^{18}$F-DOPA PET/CT to correctly detect striatal involvement. There was also a significant association ($p = 0.001$) between involvement of the dorsal striatum and its detection by $^{18}$F-DOPA PET/CT.

No significant associations were found between $^{18}$F-DOPA PET/CT-positive results and T/N ratio, tumour dimensions, grade and involvement of the ventral striatum, and no significant associations were found between $^{18}$F-DOPA PET/MRI-positive results and tumour dimensions, T/S ratio, T/N ratio and grade. However, both the univariate and multivariate analysis showed that $^{18}$F-DOPA PET/MRI perfectly predicted involvement of the dorsal striatum (all patients with involvement of the dorsal striatum were true-positive on PET/MRI). The univariate analysis also showed a statistically significant association between tumoral involvement of the ventral striatum and $^{18}$F-DOPA PET/MRI-positives results ($p = 0.04$). However, the multivariate analysis showed only a trend ($p = 0.08$). Representative MRI, PET/CT and PET/MRI images are shown in Figs. 2, 3 and 4.

## Discussion

A growing body of evidence suggests that novel amino acid PET tracers with long half-lives may have substantial advantages over FDG and methionine and add value to standard MRI for the evaluation and management of children with brain tumours [3, 4, 9–12]. $^{18}$F-DOPA and $^{18}$F-FET are emerging as the two most promising tracers, and both probes show several similarities (same half-life, similar transport mechanism) [14] with the exception of specific $^{18}$F-DOPA uptake in the putamen and caudate nucleus. Unlike with $^{18}$F-FET, this latter aspect might potentially affect the ability to

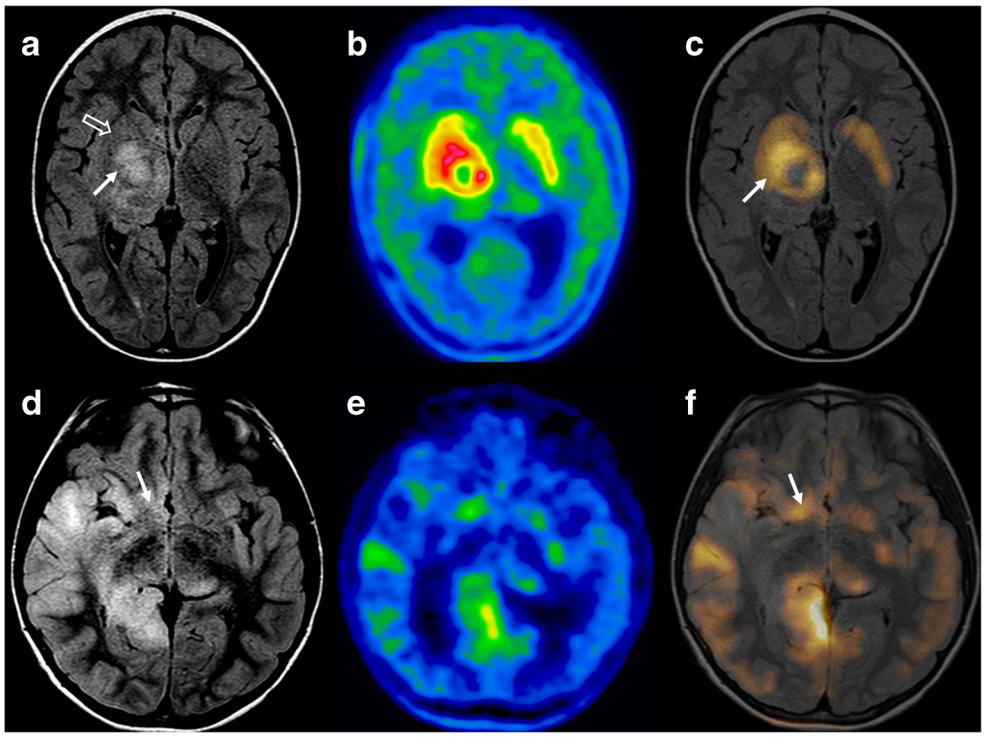


**Fig. 3** False-positive and false-negative $^{18}$F-DOPA PET/CT images. **a–c** Glioblastoma multiforme (patient 24). The axial FLAIR image (**a**) shows a right thalamic lesion with involvement of the ipsilateral internal capsule and globus pallidus (*thin arrow*). There is no evidence of involvement of the ipsilateral putamen on MRI (*open arrow*). The $^{18}$F-DOPA PET/CT image (**b**) shows increased uptake with a modified right striatal outline (discrimination between the globus pallidus and the putamen is not possible). The fused PET/MRI image (**c**) demonstrates increased uptake only in the lesion involving the right globus pallidus (*arrow*) with physiological uptake in the right putamen. **d–f** Anaplastic astrocytoma (patient 9). The axial FLAIR image (**d**) shows an extensive infiltrative lesion involving the right temporal and frontal lobes with partial involvement of the ventral striatum (*arrow*). The $^{18}$F-DOPA PET/CT image (**e**) shows patchy increased uptake in the lesion, more prominent in the right parahippocampal gyrus. On PET/CT there is no clear evidence of involvement of the striatum and in particular discrimination of the ventral striatum from the right frontal basal region is not possible. Increased spatial resolution of the fused PET/MRI image (**f**) allows increased uptake in the pathological right ventral striatum to be demonstrated in comparison with the contralateral side (*arrow*)

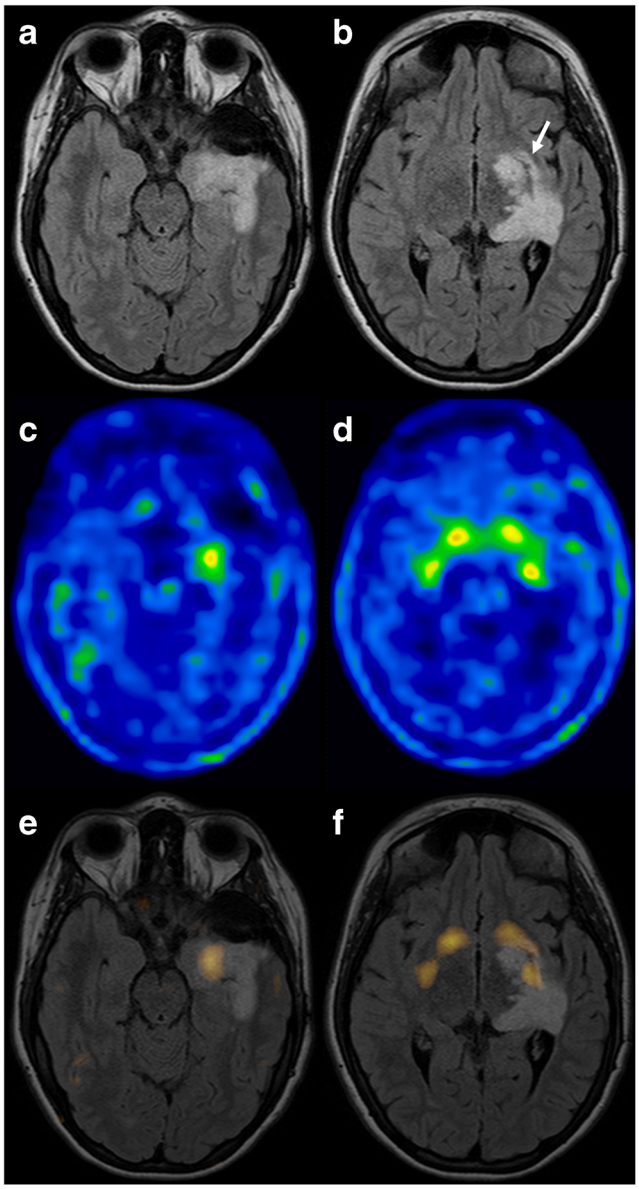


**Fig. 4** False-negative $^{18}$F-DOPA PET/CT and $^{18}$F-DOPA PET/MRI images. Ganglioglioma (patient 2). **a**, **b** The axial FLAIR images show a lesion of the left temporal lobe involving the ipsilateral ventral striatum (**b** *arrow*). **c**–**f** PET/CT images (**c**, **d**) and fused PET/MRI images (**e**, **f**) show only focally increased uptake in the lesion in the left uncal region, and do not show involvement of the ventral striatum

distinguish normal brain from adjacent tumour. On the other hand, $^{18}$F-DOPA uptake in the striatum provides the possibility to further stratify tumour uptake ratios by comparison with the uptake in both the normal background and the striatum [3].

No studies have so far compared $^{18}$F-DOPA and $^{18}$F-FET in children with brain tumours, but such a comparison has recently been performed in adults with brain glioma, at the time of diagnosis [15] and disease recurrence [16]. These studies confirmed that both tracers show comparable diagnostic results and can be successfully employed in low-grade and high-grade gliomas. However, discordant data emerged regarding the ability of $^{18}$F-DOPA PET to detect striatal involvement. Lapa et al. [15] found that despite significant basal ganglia $^{18}$F-DOPA uptake, tumour visualization was possible in all patients. In contrast, Kratochwil et al. [16] found that $^{18}$F-DOPA uptake may limit delineation of lesions close to the striatum and if there is possible involvement of the basal ganglia, $^{18}$F-FET should be preferred irrespective of tumour grade. To the best of our knowledge, no prior studies have compared $^{18}$F-DOPA PET/CT with $^{18}$F-DOPA PET/MRI and MRI to test the ability to detect tumour involvement of the basal ganglia, and Lapa et al. [15] and Kratochwil et al. [16] did not systematically compare PET/CT with fused PET/MRI. This context motivated us to perform the present study.

We excluded brain gliomas with negligible DOPA uptake from our analysis given the impossibility of evaluating the diagnostic performance in the striatum. As previously demonstrated a large percentage of low-grade paediatric diffuse astrocytomas show absent tracer uptake, reflecting the stable or slowly progressive behaviour of these lesions in children [3]. We therefore analysed a series of paediatric low-grade and high-gliomas, with and without involvement of the basal ganglia, presenting with tracer uptake in the main lesion located outside the striatum above the level of normal background (T/N ratio >1). The overall diagnostic accuracy of PET/CT was 75 % and the accuracies of MRI and PET/MRI were 100 % and 93 %, respectively. MRI was significantly more accurate ($p = 0.01$) than PET/CT but there was no significant difference between $^{18}$F-DOPA PET/MRI and MRI.

PET/CT gave two false-positive results. One was in a patient with a previously resected and treated (radiotherapy plus chemotherapy) glioblastoma who showed a small nodule of recurrent disease along the medial margin of the surgical cavity in the left temporal/parietal region. In this patient there was asymmetrically increased uptake in the putamen ipsilateral to the surgical cavity. This finding was interpreted as a sign of involvement on PET/CT, but MRI clearly showed absence of disease, and on fused PET/MRI this pattern was interpreted as a possible mechanism of persistently increased $^{18}$F-DOPA uptake following ipsilateral surgical resection. A similar finding has recently been described in an adolescent who underwent surgical resection of a hemispheric high-grade glioma and who showed persistent increased $^{18}$F-DOPA uptake in the ipsilateral putamen, possibly related to corticostriatal synaptic plasticity [17]. A follow-up MRI scan confirmed lack of disease in the striatum. The other patient showed a right mesencephalic/thalamic lesion extending to the adjacent globus pallidus. On PET/CT, discrimination between the globus pallidus and the putamen was not possible and the lesion was considered positive. In contrast the better spatial resolution of MRI and fused PET/MRI allowed correct interpretation of the involvement of the basal ganglia (Fig. 3a–c).

PET/CT gave five false-negative results, three of which were correctly detected on PET/MRI. Therefore, fused PET/

MRI was useful to rule out false-positive data and to reduce the number of false-negative results leading to a very high accuracy (93 %) in detecting involvement of the striatum, not significantly different from that of MRI. Overall, $^{18}$F-DOPA PET/MRI showed a trend towards a higher accuracy compared with $^{18}$F-DOPA PET/CT even though, probably because of the low number of events (low statistical power), statistical significance was not reached ($p = 0.06$).

The two false-negative fused PET/MRI results were two low-grade gliomas showing mildly increased uptake (T/S ratio <1) limited to focal portions of the main lesion outside the striatum. In both patients, MRI demonstrated involvement of the ventral striatum (Fig. 4) that was confirmed on follow-up. However, on fused PET/MRI, the pattern of uptake in the striatum was perfectly symmetrical without evidence of focally increased uptake or modified striatal outline matching the MRI lesion, suggesting negligible pathological DOPA uptake; therefore fused PET/MRI was not considered positive.

Different results were found for involvement of the ventral and dorsal striatum. Involvement of the dorsal striatum was detected with very high accuracy by all diagnostic tools, with 100 % accuracy for PET/MRI and 93 % accuracy for PET/CT, which gave only one false-negative result. In contrast, involvement of the ventral striatum was evaluated less accurately by PET-based modalities, and MRI was significantly more accurate than PET/CT and PET/MRI. Nevertheless, the accuracies of PET/CT and PET/MRI were 75 % and 86 %, respectively, which can still be considered good results, particularly in view of the fact that we included lesions with partial or very limited involvement of the striatum (i.e. one patient had involvement only of the nucleus accumbens) barely visible even on MRI (Fig. 3d–f).

The univariate and multivariate logistic analyses to determine which variables influenced $^{18}$F-DOPA PET/CT and $^{18}$F-DOPA PET/MRI results (tumour grade, dimensions, T/S and T/N ratios, and site of striatal involvement) showed statistically significant associations between $^{18}$F-DOPA PET/CT-positive results, T/S ratio and involvement of the dorsal striatum. Indeed all lesions with a TS ratio >1 and involvement of the dorsal striatum were true-positive on PET/CT. These findings suggest that $^{18}$F-DOPA PET/CT may fail to detect involvement of the striatum in a small percentage of patients and in particular when the T/S ratio of the main lesion is less than 1, and when the striatal involvement is limited to the ventral portion. Therefore, our qualitative analysis based on striatal uptake asymmetry and modified striatal outline appeared to be a good method for evaluating involvement of the basal ganglia. The logistic regression analysis also showed a statistically significant association between the PET/MRI results and site of striatal involvement, with a perfect prediction of involvement of the dorsal striatum. In contrast to PET/CT, the PET/MRI results did not depend on the T/S ratio, and the most plausible explanation might be because of the better spatial resolution of this diagnostic tool which allowed better detection of striatal involvement in both lesions with a T/S ratio >1 and those with a T/S ratio <1.

Limitations of our study include the relatively small sample of patients and the heterogeneity of the lesion types. However, we included only children with glioma but despite this, the number of patients included was similar or even higher than the adult series of Lapa et al. [15] and Kratochwil et al. [16]. Because we focused on the evaluation of striatal involvement, patients with diffuse astrocytoma and negligible PET uptake were not included. This aspect should be taken into account when considering the overall sensitivity and diagnostic accuracy of PET-based modalities. Another limitation concerns the standard of reference. Histological confirmation of involvement of the basal ganglia was not obtained for both practical and ethical reasons, and MRI follow-up was the standard of reference; since we considered positive even MRI lesions without contrast enhancement, detectable only on T2-weighted/FLAIR images, the possibility of false-positive MRI results should be acknowledged. However, MRI is a common standard in clinical practice and is routinely used in the follow-up of paediatric patients with brain tumours. Another limitation concerns the selection of patients included in retrospective analyses. Because not all paediatric patients with glioma at our institution undergo $^{18}$F-DOPA PET/CT imaging, interpretation of the data may have been affected by selection bias.

## Conclusion

In paediatric patients with glioma, physiological $^{18}$F-DOPA uptake in the corpus striatum does not appear to be a main limitation in the evaluation and assessment of tumours that extend into the basal ganglia. $^{18}$F-DOPA PET/CT correctly detected involvement of the dorsal striatum for lesions with a T/S ratio >1, whereas involvement of the ventral striatum was less easily evaluable. Direct comparison of $^{18}$F-DOPA PET/CT with MRI, combined with image fusion, is needed to evaluate involvement of the ventral striatum and improves diagnostic accuracy, thus its use is recommended.

### Compliance with ethical standards

**Conflicts of interest** None.

**Ethical approval** For this type of study (retrospective study) formal consent is not required. This article does not describe any studies with animals performed by any of the authors.

**Informed consent** Informed consent was signed by all patients or their legal guardians, and patient assent was obtained whenever appropriate.

## References


1. Kaplan AM, Bandy DJ, Manwaring KH, Chen K, Lawson MA, Moss SD, et al. Functional brain mapping using positron emission tomography scanning in preoperative neurosurgical planning for pediatric brain tumors. J Neurosurg. 1999;91:797–803.
2. Pirotte B, Goldman S, Salzberg S, Wikler D, David P, Vandesteene A, et al. Combined positron emission tomography and magnetic resonance imaging for the planning of stereotactic brain biopsies in children: experience in 9 cases. Pediatr Neurosurg. 2003;38:146–55.
3. Morana G, Piccardo A, Milanaccio C, Puntoni M, Nozza P, Cama A, et al. Value of 18F-3,4-dihydroxyphenylalanine PET/MR image fusion in pediatric supratentorial infiltrative astrocytomas: a prospective pilot study. J Nucl Med. 2014;55:718–23.
4. Morana G, Piccardo A, Garrè ML, Nozza P, Consales A, Rossi A. Multimodal magnetic resonance imaging and 18F-L-dihydroxyphenylalanine positron emission tomography in early characterization of pseudoresponse and nonenhancing tumor progression in a pediatric patient with malignant transformation of ganglioglioma treated with bevacizumab. J Clin Oncol. 2013;31:e1–5.
5. Piccardo A, Lopci E, Conte M, Garaventa A, Foppiani L, Altrinetti V, et al. Comparison of 18F-DOPA PET/CT and 123IMIBG scintigraphy in stage 3 and 4 neuroblastoma: a pilot study. Eur J Nucl Med Mol Imaging. 2012;39:57–71.
6. Piccardo A, Puntoni M, Lopci E, Conte M, Foppiani L, Sorrentino S, et al. Prognostic value of 18F-DOPA PET/CT at the time of recurrence in patients affected by neuroblastoma. Eur J Nucl Med Mol Imaging. 2014;41:1046–56.
7. Piccardo A, Morana G, Massollo M, Pescetto M, Conte M, Garaventa A. Brain metastasis from neuroblastoma depicted by 18F-DOPA PET/CT. Nucl Med Mol Imaging. 2015;49:241–2. doi:10.1007/s13139-015-0322-8.
8. Ribeiro MJ, De Lonlay P, Delzescaux T, Boddaert N, Jaubert F, Bourgeois S, et al. Characterization of hyperinsulinism in infancy assessed with PET and 18F-fluoro-L-DOPA. J Nucl Med. 2005;46:560–6.
9. Morana G, Piccardo A, Puntoni M, Nozza P, Cama A, Raso A, et al. Diagnostic and prognostic value of 18F-DOPA PET and 1H-MR spectroscopy in pediatric supratentorial infiltrative gliomas: a comparative study. Neuro Oncol. 2015;17:1637–47.
10. Misch M, Guggemos A, Driever PH, Koch A, Grosse F, Steffen IG, et al. (18)F-FET-PET guided surgical biopsy and resection in children and adolescence with brain tumors. Childs Nerv Syst. 2015;31:261–7.
11. Dunkl V, Cleff C, Stoffels G, Judov N, Sarikaya-Seiwert S, Law I, et al. The usefulness of dynamic O-(2-18F-fluoroethyl)-L-tyrosine PET in the clinical evaluation of brain tumors in children and adolescents. J Nucl Med. 2015;56:88–92.
12. Fraioli F, Shankar A, Hargrave D, Hyare H, Gaze MN, Groves AM, et al. 18F-fluoroethylcholine (18F-Cho) PET/MRI functional parameters in pediatric astrocytic brain tumors. Clin Nucl Med. 2015;40:e40–5.
13. Porter JN, Roy AK, Benson B, Carlisi C, Collins PF, Leibenluft E, et al. Age-related changes in the intrinsic functional connectivity of the human ventral vs. dorsal striatum from childhood to middle age. Dev Cogn Neurosci. 2015;11:83–95.
14. Galldiks N, Langen KJ, Pope WB. From the clinician's point of view – What is the status quo of positron emission tomography in patients with brain tumors? Neuro Oncol. 2015;17:1434–44.
15. Lapa C, Linsenmann T, Monoranu CM, Samnick S, Buck AK, Bluemel C, et al. Comparison of the amino acid tracers 18F-FET and 18F-DOPA in high-grade glioma patients. J Nucl Med. 2014;55:1611–6.
16. Kratochwil C, Combs SE, Leotta K, Afshar-Oromieh A, Rieken S, Debus J, et al. Intra-individual comparison of 18F-FET and 18F-DOPA in PET imaging of recurrent brain tumors. Neuro Oncol. 2014;16:434–40.
17. Morana G, Piccardo A, Garrè ML, Nobili F, Rossi A. Late persistent increased putaminal 18F-DOPA uptake following ipsilateral frontal resection: evidence for corticostriatal synaptic plasticity? Clin Nucl Med. 2015;40:e451–2.